Spectroscopy of Spin-Split Andreev Levels in a Quantum Dot with Superconducting Leads

Arno Bargerbos,[1,*] Marta Pita-Vidal,[1,*] Rok Žitko,[2,3] Lukas J. Splitthoff,[1] Lukas Grünhaupt,[1] Jaap J. Wesdorp,[1] Yu Liu,[4] Leo P. Kouwenhoven,[1] Ramón Aguado,[5] Christian Kraglund Andersen,[1] Angela Kou,[6] and Bernard van Heck[7,8]

[1]QuTech and Kavli Institute of Nanoscience, Delft University of Technology, 2600 GA Delft, Netherlands
[2]Jožef Stefan Institute, Jamova 39, SI-1000 Ljubljana, Slovenia
[3]Faculty of Mathematics and Physics, University of Ljubljana, Jadranska 19, SI-1000 Ljubljana, Slovenia
[4]Center for Quantum Devices, Niels Bohr Institute, University of Copenhagen, 2100 Copenhagen, Denmark
[5]Instituto de Ciencia de Materiales de Madrid (ICMM), Consejo Superior de Investigaciones Cientificas (CSIC), Sor Juana Ines de la Cruz 3, 28049 Madrid, Spain
[6]Department of Physics and Frederick Seitz Materials Research Laboratory, University of Illinois Urbana-Champaign, Urbana, Illinois 61801, USA
[7]Leiden Institute of Physics, Leiden University, Niels Bohrweg 2, 2333 CA Leiden, Netherlands
[8]Dipartimento di Fisica, Università di Roma "La Sapienza", P.le Aldo Moro 5, 00185 Roma, Italy

(Received 28 August 2022; accepted 27 July 2023; published 31 August 2023)

We use a hybrid superconductor-semiconductor transmon device to perform spectroscopy of a quantum dot Josephson junction tuned to be in a spin-1/2 ground state with an unpaired quasiparticle. Because of spin-orbit coupling, we resolve two flux-sensitive branches in the transmon spectrum, depending on the spin of the quasiparticle. A finite magnetic field shifts the two branches in energy, favoring one spin state and resulting in the anomalous Josephson effect. We demonstrate the excitation of the direct spin-flip transition using all-electrical control. Manipulation and control of the spin-flip transition enable the future implementation of charging energy protected Andreev spin qubits.

DOI: 10.1103/PhysRevLett.131.097001

In the confined geometry of a Josephson junction, the Andreev reflection of an electron into a hole at a normal-superconducting interface results in discrete Andreev bound states (ABSs) [1–6]. ABSs are a fundamental part of mesoscopic superconductivity and the basis of several qubit proposals [7–10]. In particular, an ABS populated by a single quasiparticle can serve as the superconducting version of a spin qubit. Because of spin-orbit interaction, the Josephson phase difference ϕ couples the spin to the supercurrent, breaking the spin degeneracy [9,11]. This allows for direct integration of spin qubits into superconducting circuits for remote communication, transduction, or hybrid qubit platforms [12–14].

Measurements of InAs/Al nanowire Josephson junctions revealed the predicted spin-split ABSs [15–17], leading to the demonstration of coherent Andreev spin qubit manipulation [18]. In these remarkable experiments, the spin-1/2 states were an excited manifold and thus susceptible to qubit leakage via quasiparticle escape or recombination, bringing the junction back into its spin-zero ground state. Furthermore, direct spin manipulation proved unfeasible, likely due to the smallness of relevant matrix elements [19], requiring excitation schemes involving auxiliary levels [18,20].

Recently [21], we showed that embedding a gate-controlled quantum dot in the InAs/Al junction allows tuning it to have an odd-parity spin-1/2 ground state. In this doublet phase, the lifetime of the trapped quasiparticle can exceed 1 ms, likely benefiting from the charging energy of the quantum dot suppressing quasiparticle poisoning events.

In this Letter, employing the same transmon techniques as in Ref. [21], we report the detection of the spin-orbit-induced spin splitting of ABSs in a quantum dot Josephson junction. The energy difference between spin states is smaller than the electron temperature, which would hinder its detection in transport measurements. The spin-split state populations and the spin-selective transmon frequencies can be controlled via external magnetic fields smaller than 40 mT. Furthermore, in the presence of magnetic field, we observe the anomalous Josephson effect: a shift of the energy-phase relation minimum to a value ϕ_0 different from 0 or π, or, equivalently, the presence of a nonzero equilibrium supercurrent at $\phi = 0$ [22–25]. Finally, we show that the spin can be directly manipulated by applying microwaves to a bottom gate, via the electric dipole spin resonance (EDSR) [26–31]. Our experiment is comparable to, and inspired by, the theoretical proposal of Ref. [10], which we use to model the data, combined with further understanding based on a modified single-impurity Anderson model (SIAM).

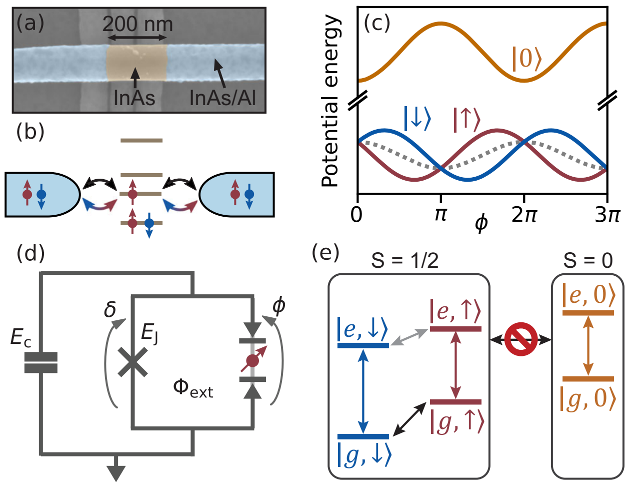

FIG. 1. (a) False-colored scanning electron micrograph of the quantum dot junction. (b) Diagram of a quantum dot junction with multiple energy levels. Black (blue to red) arrows denote the spin-conserving (spin-flipping) tunnel couplings. (c) Josephson potential $U(\phi)$ for the singlet state (orange line) and the two doublet states (red and blue lines). The dotted gray line represents the latter without the E_{SO} term. (d) Circuit model for a transmon with charging energy E_c and a grounded SQUID formed by the parallel combination of a quantum dot junction and a reference Josephson junction with Josephson energy E_J. δ denotes the phase difference across the reference junction and Φ_{ext} is the external magnetic flux through the SQUID loop. (e) Diagram of the joint transmon-quantum dot junction energy levels. The transmon transition frequencies $|g\rangle \leftrightarrow |e\rangle$ (vertical arrows) depend on the quantum dot junction state. Coherent microwave transitions between singlet and doublet are forbidden. However, intradoublet spin-flip transitions are possible (diagonal arrows).

The core of our experiment is a quantum dot Josephson junction hosted in a nominally 10-μm-long InAs/Al superconductor-semiconductor nanowire with a 110-nm-wide hexagonal core and a 6-nm-thick shell covering two facets [32]. The quantum dot is electrostatically defined in a 200-nm-long wet-etched InAs section using three bottom gates with voltages V_L, V_C, and V_R. Its superconducting leads are formed by the flanking InAs/Al sections [Fig. 1(a)]. The bottom gates can be used to control the occupation of the quantum dot and its coupling to the superconducting leads, resulting in two possible ground states of the quantum dot junction: either a spin-zero or a spin-1/2 state. We are particularly interested in the latter case [Fig. 1(b)], where the ground state manifold is spanned by the two components, $|\downarrow\rangle$ and $|\uparrow\rangle$, of a Kramers doublet, and a minimal model for the potential energy of the junction is given by [10]

$$U(\phi) = E_0 \cos(\phi) - E_{SO}\vec{\sigma} \cdot \vec{n} \sin(\phi) + \frac{1}{2}\vec{E}_Z \cdot \vec{\sigma}. \quad (1)$$

Here, $\vec{\sigma}$ is the spin operator, $\vec{n}$ is a unit vector along the spin-polarization direction set by the spin-orbit interaction, and E_{SO} and E_0 are spin-dependent and spin-independent Cooper pair tunneling rates, respectively. Note that the E_0 term has a minimum at $\phi = \pi$. This π shift originates from the odd occupancy of the junction [33,34] and distinguishes the Josephson energy from that of a conventional tunnel junction. Finally, $\vec{E}_Z$ is a Zeeman field arising in the presence of an external magnetic field.

The energies E_0 and E_{SO} can be understood as follows [10]. Cooper pair tunneling occurs via a sequence of single-electron cotunneling processes through the quantum dot energy levels. The spin-independent component E_0 arises from those sequences in which both electrons cotunnel through the same energy level. The amplitude for these sequences is the same whether the initial state of the quantum dot junction is $|\downarrow\rangle$ or $|\uparrow\rangle$. On the other hand, E_{SO} arises from tunneling processes in which one electron cotunnels through the singly occupied level, involving a spin rotation, while the second one cotunnels through a different level. Since in the presence of spin-orbit coupling the single-electron tunneling amplitudes can be spin dependent, for these processes the *pair* tunneling amplitude may depend on the spin of the initial state.

The two potential energy branches of the doublet states at $\vec{E}_Z = \vec{0}$, $E_{\downarrow,\uparrow} = E_0 \cos\phi \pm E_{SO} \sin\phi$, are sinusoidals with an amplitude of $\sqrt{E_0^2 + E_{SO}^2}$ and minima at $\phi_0 = \pi \pm \arctan(E_{SO}/E_0)$; see Fig. 1(c). If $E_{SO} = 0$, the potential energy reduces to the π-junction behavior without spin splitting. At nonzero E_{SO}, the shift of the minima away from $\phi = 0, \pi$ is a precursor [10] to the anomalous Josephson effect [22,23]; while at $\phi = 0$ there will be instantaneous supercurrents on timescales short compared to the spin lifetime, the time-averaged current will be zero due to thermal fluctuations. In Fig. 1(c) we also show the potential energy E_s of the lowest-energy singlet state $|0\rangle$, with a minimum at $\phi = 0$, as expected for a conventional Josephson junction.

We derive the occurrence of both E_0 and E_{SO} within a minimally extended SIAM with superconducting leads. The SIAM is a simple model widely used to understand quantum dot junctions, containing a single energy level coupled to the leads via spin-conserving tunneling events [33,35–43]. Two extensions to the SIAM are required to generate the spin-splitting term E_{SO}: (i) spin-flipping single-electron tunneling between the leads and the energy level [10,14,44,45] and (ii) interlead tunneling, resulting from integrating out additional quantum dot energy levels. These results are derived in Ref. [46], together with a validation based on numerical renormalization group calculations.

In view of the strong spin-orbit coupling in InAs [60,61] and the confinement on the order of 100 nm [62–64], we expect both spin-flipping and spin-conserving tunneling, as well as additional quantum dot levels, to be present in our device. Note that within this model, the energy E_0 in Eq. (1) may have either sign. While both situations may occur at

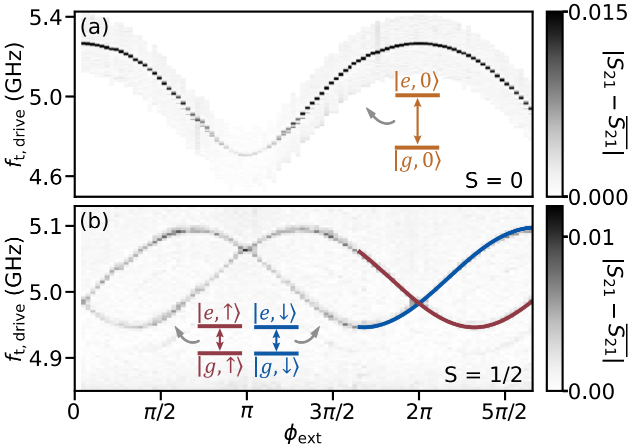

FIG. 2. Comparison of transmon two-tone spectroscopy taken with either a singlet (a) or a spin-split doublet ground state (b). Both panels show the transmitted microwave signal versus external flux, ϕ_{ext}, and transmon drive frequency $f_{\mathrm{t,drive}}$. The two ground states occur for two different gate voltage settings, as detailed in Refs. [21,46]. Solid lines show fits to a transmon circuit model containing Eq. (1) [46].

different gate settings in the same device, the tuning procedure to find a doublet ground state relies on the detection of a π shift [21]. Thus, our experiment naturally selects the case $E_0 > 0$, justifying the sign choice in Eq. (1).

To resolve the predicted spin splitting we incorporate the quantum dot junction into the superconducting quantum interference device (SQUID) of a transmon circuit [Fig. 1(d)] [65], as done in Ref. [21]. The different potential energies corresponding to the states $|0\rangle$, $|\downarrow\rangle$, or $|\uparrow\rangle$ give rise to distinct transmon transition frequencies [Fig. 1(e)], which can be detected and distinguished via standard microwave techniques [66,67].

To study the system in the regime of interest, we tune the quantum dot junction to a setpoint with a spin-1/2 ground state (gate setpoint A [68]), as detailed in Ref. [46]. This is followed by a two-tone spectroscopy measurement for which we apply both tones through the feedline and detect the transmon frequency as a function of the applied flux Φ_{ext}. The flux is tuned with a small in-plane external magnetic field applied perpendicular to the wire [69], requiring a 1.8 mT field for adding one flux quantum through the SQUID. Since the reference junction is tuned to have a Josephson energy $E_{\mathrm{J}}/h = 12.5$ GHz, much higher than that of the quantum dot junction, the phase difference across the latter is well approximated by $\phi_{\mathrm{ext}} = 2e\Phi_{\mathrm{ext}}/\hbar$.

In Fig. 2(a), we show the typical flux dispersion observed in two-tone spectroscopy when the gate voltages are such that the ground state is a singlet, with the maximum frequency occurring at $\phi_{\mathrm{ext}} = 0$. In fact, this measurement serves as a calibration of the applied flux, which is assumed to be an integer multiple of the flux quantum when the transmon frequency is maximal. In contrast, when the ground state is electrostatically set to be a doublet, the transition spectrum displays two shifted frequency branches, with maxima at $\phi_{\mathrm{ext}} = \phi_0 \neq 0, \pi$ [Fig. 2(b)]. The measured spectrum is in agreement with that predicted by a transmon circuit model with the potential energy of Eq. (1), with $E_0/h = 190$ MHz, $E_{\mathrm{SO}}/h = 300$ MHz, $E_{\mathrm{J}}/h = 12.5$ GHz, and $E_{\mathrm{c}}/h = 284$ MHz [46]. The latter corresponds to a temperature scale of 14 mK, indicating that transmon-based spectroscopy can experimentally resolve the spin-orbit splitting of the doublet state below the thermal broadening that limits tunneling spectroscopy experiments.

We note that a spin-1/2 ground state is not a sufficient condition to observe the spin splitting. By tuning the quantum dot to different resonances, corresponding to a quasiparticle trapped to different levels of the quantum dot, we frequently find instances of doublets without the predicted splitting, such as the one studied in detail in Ref. [21]. There are also doublet states that show a small, MHz-size, spin splitting comparable to the transmon linewidth, as well as with larger splittings than shown in Fig. 2(b). This range of behaviors is shown in Ref. [46]. We attribute this variability to mesoscopic fluctuations [10], due to factors outside of our experimental control, such as disorder and confinement effects on the quantum dot wave functions.

The transition spectrum is affected by magnetic field through the Zeeman interaction and depends sensitively on the field direction with respect to the spin-orbit direction $\vec{n}$. This is shown in Fig. 3, which shows two limiting cases: $B_{\parallel}$, the direction along $\vec{n}$, and $B_{\perp}$, the direction perpendicular to $\vec{n}$. The evolution for intermediate directions and the procedure used to infer $\vec{n}$ are discussed in Ref. [46]. The flux dispersion of the transition frequencies is only weakly affected by increasing $B_{\parallel}$ [70]. Moreover, one of the two spin branches gradually disappears [Fig. 3(a)] until at $B_{\parallel} \gtrsim 23$ mT only a single spectroscopic line remains visible [Fig. 3(b)]. In this regime, the minimum transmon transition frequency of the single-valued dispersion is shifted by ϕ_0 away from $\phi_{\mathrm{ext}} = 0$. This is a consequence of a ϕ_0 shift of the maximum of the energy-phase relation away from $\phi = 0$, as the transmon transition frequency is given by the Josephson inductance, the second derivative of the energy-phase relationship. This observation therefore demonstrates the presence of the anomalous Josephson effect [22–25,72]. In contrast, increasing the magnetic field along the $B_{\perp}$ direction appears to couple the two spectroscopic lines, leading to branches with two minima per flux period [Fig. 3(c)]. At even higher fields this behavior is lifted, and only one of the two transmon branches persists [Fig. 3(d)]. In this case, however, the ϕ_0 offset has strongly decreased.

These observations can be understood from Eq. (1) by considering a Zeeman field parallel or perpendicular to the spin-orbit direction. A parallel field $E_{\mathrm{Z}}^{\parallel}$ separates the

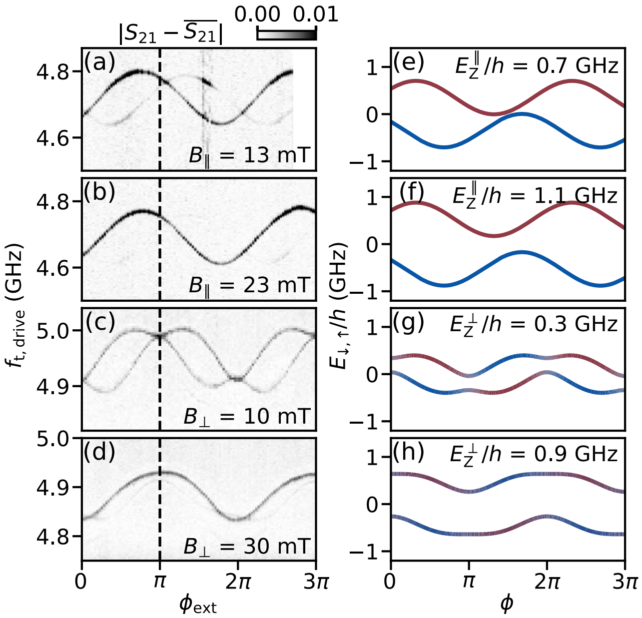

FIG. 3. Magnetic field dependence of the doublet states (gate setpoint A). (a)–(d) Transmon spectroscopy versus ϕ_{ext} for a magnetic field applied either parallel (a), (b) or perpendicular (c), (d) to the inferred spin-orbit direction $\vec{n}$ [73]. (e), (f) Numerically calculated Josephson potential for the two doublet states, obtained by diagonalizing Eq. (1), with either parallel (e), (f) or perpendicular (g), (h) Zeeman field. Blue and red colors denote $|\downarrow\rangle$ and $|\uparrow\rangle$ spin polarization, respectively, with a blend of the two indicating mixing of the states. Panels (e)–(h) are not fits to the data of (a)–(d). Instead, together with the contribution from the reference junction, constitute the potentials that determine the transmon energy levels and serve to build a qualitative understanding (see text).

doublet potentials in energy without distorting their phase dependence [Figs. 3(e) and 3(f)]. As the energy separation increases, the thermal population of the higher-energy state decreases and, with it, so does the visibility of the corresponding transmon frequency branch. As the transmon frequency is insensitive to overall shifts in the energy-phase relation, it is unaffected by the ϕ-independent field-induced energy shift. A Zeeman term $E_Z^\perp$ perpendicular to the spin-orbit direction instead couples the two states and opens up an avoided crossing in the Josephson potential [Fig. 3(g)]. This results in the peculiar flux dependence seen in spectroscopy for moderate fields [Fig. 3(c)]. Finally, when $E_Z^\perp$ becomes much larger than E_{SO}, the doublet states polarize along the applied field direction [Fig. 3(h)], suppressing the ϕ_0 offset [22,25].

We find that the $\vec{n}$ direction is not clearly related to the orientation of the nanowire: it points 13 deg away from the nanowire axis. Moreover, this direction is found to be unique to each region in gate space [46]. This behavior differs from that of long single-gated semiconducting Josephson junctions, where the $\vec{n}$ direction is perpendicular to the nanowire axis [15,74]. As the direction $\vec{n}$ is dictated

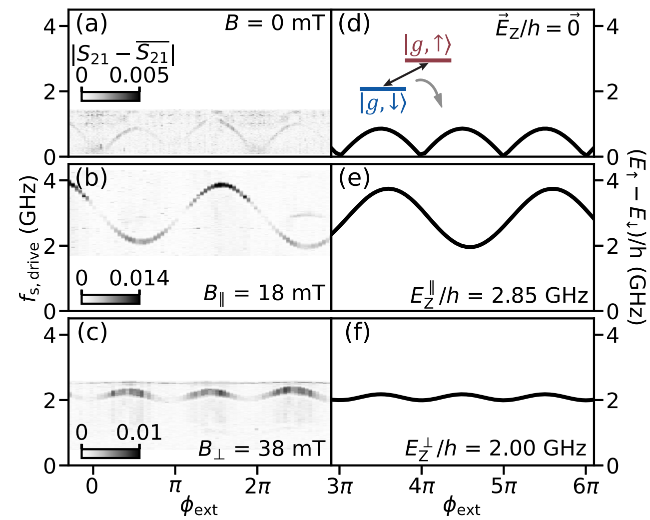

FIG. 4. Direct spin-flip spectroscopy for gate setpoint B. (a)–(c) Measured flux dependence of the direct $|g,\downarrow\rangle \leftrightarrow |g,\uparrow\rangle$ transition frequency for no (a), parallel (b), and perpendicular (c) magnetic field relative to $\vec{n}$. (d)–(f) Numerically calculated flux dependence of the $|g,\downarrow\rangle \leftrightarrow |g,\uparrow\rangle$ transition frequency for no (d), parallel (e), and perpendicular (f) Zeeman fields relative to $\vec{n}$.

by the averaged electric field in the junction region where the Andreev bound state wave function is situated, we attribute this variability to mesoscopic fluctuations of the electrostatic potential landscape when the gate setpoint is changed [75].

To use the doublet states as a superconducting spin qubit [9,10], the ability to drive transitions between the doublet states is crucial. A recent work by our group indicates that spin-flip transitions of ABS are possible in the presence of an external magnetic field [69]. Motivated by all-electrical microwave excitation of spins in quantum dots via EDSR [29,30], we apply a microwave tone directly to the central gate to excite the doublet states. For this, we tune the transmon frequency close to the resonator frequency, enhancing its dispersive shift. In addition, we tune away from the gate setpoint investigated so far (gate setpoint A) to a parameter regime with a larger spin splitting $E_{\mathrm{SO}}/h =$ 560 MHz (gate setpoint B) to maximize the visibility of the doublet splitting [46].

Applying a microwave drive to the central gate electrode, we find that a low-frequency transition of up to 1 GHz can be detected for a vanishing applied magnetic field [76], as also shown in Ref. [17] [Fig. 4(a)]. Its poor visibility is potentially due to the lack of magnetic field, which reduces the efficacy of EDSR [27,28], as well as to the large thermal population of the excited state, which reduces the achievable change in dispersive shift. This large thermal population can be expected from the fact that the spin-flip transition energy corresponds to an effective temperature range of 0–50 mK, below the typical electron temperatures found in transport and transmon [77] experiments, 35–100 mK. At elevated $B_\parallel$

the transition frequency rises and becomes well resolved [Fig. 4(b)]. For an applied perpendicular field the transition frequency increases more slowly, and its flux periodicity is half that of the transition in the parallel field direction [Fig. 4(c)]. Note that the $\vec{n}$ direction found for gate setpoint B (72 deg away from the nanowire axis [46]) differs from that of gate setpoint A, and that therefore $B_{\parallel}$ and $B_{\perp}$ in Fig. 4 point in different directions than in Fig. 3.

The observed behavior is consistent with the expected transitions between the doublet states [Figs. 4(d)–4(f)], with the period halving in perpendicular field being a result of the avoided crossings between the spin branches [cf. Fig. 3(g)]. The comparison to the model furthermore allows us to estimate the effective g factors in the parallel and perpendicular directions, $g_{\parallel} = 11$ and $g_{\perp} = 3.8$, respectively. These values depend strongly on the gate voltages [46], likely tied to an interplay of spin-orbit coupling and confinement, beyond the scope of the model considered here [78–81].

To conclude, our microwave measurements have revealed the spin structure of energy levels in a quantum dot Josephson junction and the occurrence of the anomalous Josephson effect. These findings are promising for applications in superconducting spintronics [82,83]. The ability to drive spin-flip transitions between the doublet states is encouraging for the nascent field of Andreev spin qubits [9,10], since direct, all-electrical access to these transitions promises simpler and faster qubit manipulation [30,31]. Furthermore, the polarization of the doublet states at elevated magnetic fields eliminates the unwanted excited state population observed previously [16,18]. Finally, the demonstrated field or flux tunability of the transition frequency is a necessary ingredient for scalable networks of such qubits [14].

The data and analysis code that support the findings of this study are openly available in 4TU.ResearchData [84].

We acknowledge fruitful discussion with Yuli Nazarov and Valla Fatemi. We thank Peter Krogstrup for guidance in the material growth. This research is cofunded by the allowance for Top consortia for Knowledge and Innovation (TKI's) from the Dutch Ministry of Economic Affairs, research project *Scalable circuits of Majorana qubits with topological protection* (i39, SCMQ) with Project No. 14SCMQ02, from the Dutch Research Council (NWO), and the Microsoft Quantum initiative. R. Ž. acknowledges the support of the Slovenian Research agency (ARRS) under P1-0416 and J1-3008. R. A. acknowledges support from the Spanish Ministry of Science and Innovation through Grants No. PGC2018-097018-B-I00 and No. PID2021-125343NB-I00 and from the CSIC Research Platform on Quantum Technologies PTI-001. C. K. A additionally acknowledges support from the Dutch Research Council (NWO). B. v. H. was partially supported by the Dutch Research Council (NWO).

*These authors contributed equally to this work.

[1] I. Kulik, Macroscopic quantization and the proximity effect in SNS junctions, Sov. J. Exp. Theor. Phys. **30**, 944 (1969), http://www.jetp.ras.ru/cgi-bin/dn/e_030_05_0944.pdf.

[2] A. Furusaki and M. Tsukada, A unified theory of clean Josephson junctions, Physica B (Amsterdam) **165–166**, 967 (1990).

[3] C. W. J. Beenakker, Universal Limit of Critical-Current Fluctuations in Mesoscopic Josephson Junctions, Phys. Rev. Lett. **67**, 3836 (1991).

[4] P. F. Bagwell, Suppression of the Josephson current through a narrow, mesoscopic, semiconductor channel by a single impurity, Phys. Rev. B **46**, 12573 (1992).

[5] L. Bretheau, Ç. Girit, H. Pothier, D. Esteve, and C. Urbina, Exciting Andreev pairs in a superconducting atomic contact, Nature (London) **499**, 312 (2013).

[6] J. A. Sauls, Andreev bound states and their signatures, Phil. Trans. R. Soc. A **376**, 20180140 (2018).

[7] M. A. Despósito and A. L. Yeyati, Controlled dephasing of Andreev states in superconducting quantum point contacts, Phys. Rev. B **64**, 140511(R) (2001).

[8] A. Zazunov, V. S. Shumeiko, E. N. Bratus', J. Lantz, and G. Wendin, Andreev Level Qubit, Phys. Rev. Lett. **90**, 087003 (2003).

[9] N. M. Chtchelkatchev and Y. V. Nazarov, Andreev Quantum Dots for Spin Manipulation, Phys. Rev. Lett. **90**, 226806 (2003).

[10] C. Padurariu and Y. V. Nazarov, Theoretical proposal for superconducting spin qubits, Phys. Rev. B **81**, 144519 (2010).

[11] B. Béri, J. H. Bardarson, and C. W. J. Beenakker, Splitting of Andreev levels in a Josephson junction by spin-orbit coupling, Phys. Rev. B **77**, 045311 (2008).

[12] N. Lauk, N. Sinclair, S. Barzanjeh, J. P. Covey, M. Saffman, M. Spiropulu, and C. Simon, Perspectives on quantum transduction, Quantum Sci. Technol. **5**, 020501 (2020).

[13] R. Aguado, A perspective on semiconductor-based superconducting qubits, Appl. Phys. Lett. **117**, 240501 (2020).

[14] M. Spethmann, X.-P. Zhang, J. Klinovaja, and D. Loss, Coupled superconducting spin qubits with spin-orbit interaction, Phys. Rev. B **106**, 115411 (2022).

[15] L. Tosi, C. Metzger, M. F. Goffman, C. Urbina, H. Pothier, S. Park, A. L. Yeyati, J. Nygård, and P. Krogstrup, Spin-Orbit Splitting of Andreev States Revealed by Microwave Spectroscopy, Phys. Rev. X **9**, 011010 (2019).

[16] M. Hays, V. Fatemi, K. Serniak, D. Bouman, S. Diamond, G. de Lange, P. Krogstrup, J. Nygård, A. Geresdi, and M. H. Devoret, Continuous monitoring of a trapped superconducting spin, Nat. Phys. **16**, 1103 (2020).

[17] C. Metzger, S. Park, L. Tosi, C. Janvier, A. A. Reynoso, M. F. Goffman, C. Urbina, A. Levy Yeyati, and H. Pothier, Circuit-QED with phase-biased Josephson weak links, Phys. Rev. Res. **3**, 013036 (2021).

[18] M. Hays, V. Fatemi, D. Bouman, J. Cerrillo, S. Diamond, K. Serniak, T. Connolly, P. Krogstrup, J. Nygård, A. Levy Yeyati, A. Geresdi, and M. H. Devoret, Coherent manipulation of an Andreev spin qubit, Science **373**, 430 (2021).

[19] S. Park and A. L. Yeyati, Andreev spin qubits in multichannel Rashba nanowires, Phys. Rev. B **96**, 125416 (2017).

[20] J. Cerrillo, M. Hays, V. Fatemi, and A. L. Yeyati, Spin coherent manipulation in Josephson weak links, Phys. Rev. Res. **3**, L022012 (2021).

[21] A. Bargerbos, M. Pita-Vidal, R. Žitko, J. Ávila, L. J. Splitthoff, L. Grünhaupt, J. J. Wesdorp, C. K. Andersen, Y. Liu, L. P. Kouwenhoven, R. Aguado, A. Kou, and B. van Heck, Singlet-doublet transitions of a quantum dot Josephson junction detected in a transmon circuit, PRX Quantum **3**, 030311 (2022).

[22] A. Zazunov, R. Egger, T. Jonckheere, and T. Martin, Anomalous Josephson Current through a Spin-Orbit Coupled Quantum Dot, Phys. Rev. Lett. **103**, 147004 (2009).

[23] A. Brunetti, A. Zazunov, A. Kundu, and R. Egger, Anomalous Josephson current, incipient time-reversal symmetry breaking, and Majorana bound states in interacting multilevel dots, Phys. Rev. B **88**, 144515 (2013).

[24] T. Yokoyama, M. Eto, and Y. V. Nazarov, Anomalous Josephson effect induced by spin-orbit interaction and Zeeman effect in semiconductor nanowires, Phys. Rev. B **89**, 195407 (2014).

[25] D. B. Szombati, S. Nadj-Perge, D. Car, S. R. Plissard, E. P. A. M. Bakkers, and L. P. Kouwenhoven, Josephson ϕ_0-junction in nanowire quantum dots, Nat. Phys. **12**, 568 (2016).

[26] E. I. Rashba and A. L. Efros, Orbital Mechanisms of Electron-Spin Manipulation by an Electric Field, Phys. Rev. Lett. **91**, 126405 (2003).

[27] C. Flindt, A. S. Sørensen, and K. Flensberg, Spin-Orbit Mediated Control of Spin Qubits, Phys. Rev. Lett. **97**, 240501 (2006).

[28] V. N. Golovach, M. Borhani, and D. Loss, Electric-dipole-induced spin resonance in quantum dots, Phys. Rev. B **74**, 165319 (2006).

[29] K. C. Nowack, F. H. L. Koppens, Y. V. Nazarov, and L. M. K. Vandersypen, Coherent control of a single electron spin with electric fields, Science **318**, 1430 (2007).

[30] S. Nadj-Perge, S. M. Frolov, E. P. A. M. Bakkers, and L. P. Kouwenhoven, Spin–orbit qubit in a semiconductor nanowire, Nature (London) **468**, 1084 (2010).

[31] J. W. G. van den Berg, S. Nadj-Perge, V. S. Pribiag, S. R. Plissard, E. P. A. M. Bakkers, S. M. Frolov, and L. P. Kouwenhoven, Fast Spin-Orbit Qubit in an Indium Antimonide Nanowire, Phys. Rev. Lett. **110**, 066806 (2013).

[32] P. Krogstrup, N. L. B. Ziino, W. Chang, S. M. Albrecht, M. H. Madsen, E. Johnson, J. Nygård, C. Marcus, and T. S. Jespersen, Epitaxy of semiconductor-superconductor nanowires, Nat. Mater. **14**, 400 (2015).

[33] L. I. Glazman and K. A. Matveev, Resonant Josephson current through Kondo impurities in a tunnel barrier, JETP Lett. **49**, 570 (1989), http://jetpletters.ru/ps/1121/article_16988.pdf.

[34] B. I. Spivak and S. A. Kivelson, Negative local superfluid densities: The difference between dirty superconductors and dirty Bose liquids, Phys. Rev. B **43**, 3740 (1991).

[35] T. Yoshioka and Y. Ohashi, Numerical renormalization group studies on single impurity Anderson model in superconductivity: A unified treatment of magnetic, nonmagnetic impurities, and resonance scattering, J. Phys. Soc. Jpn. **69**, 1812 (2000).

[36] M.-S. Choi, M. Lee, K. Kang, and W. Belzig, Kondo effect and Josephson current through a quantum dot between two superconductors, Phys. Rev. B **70**, 020502(R) (2004).

[37] A. Oguri, Y. Tanaka, and A. C. Hewson, Quantum phase transition in a minimal model for the Kondo effect in a Josephson junction, J. Phys. Soc. Jpn. **73**, 2494 (2004).

[38] Y. Tanaka, A. Oguri, and A. C. Hewson, Kondo effect in asymmetric Josephson couplings through a quantum dot, New J. Phys. **9**, 115 (2007).

[39] A. Martín-Rodero and A. Levy Yeyati, Josephson and Andreev transport through quantum dots, Adv. Phys. **60**, 899 (2011).

[40] C. Karrasch, A. Oguri, and V. Meden, Josephson current through a single Anderson impurity coupled to BCS leads, Phys. Rev. B **77**, 024517 (2008).

[41] D. J. Luitz, F. F. Assaad, T. Novotný, C. Karrasch, and V. Meden, Understanding the Josephson Current through a Kondo-Correlated Quantum Dot, Phys. Rev. Lett. **108**, 227001 (2012).

[42] A. Kadlecová, M. Žonda, V. Pokorný, and T. Novotný, Practical Guide to Quantum Phase Transitions in Quantum-Dot-Based Tunable Josephson Junctions, Phys. Rev. Appl. **11**, 044094 (2019).

[43] V. Meden, The Anderson–Josephson quantum dot—A theory perspective, J. Phys. Condens. Matter **31**, 163001 (2019).

[44] J. Danon and Y. V. Nazarov, Pauli spin blockade in the presence of strong spin-orbit coupling, Phys. Rev. B **80**, 041301(R) (2009).

[45] H. Barakov and Y. V. Nazarov, Supercurrent in the presence of direct transmission and a resonant localized state, arXiv:2201.07848.

[46] See Supplemental Material at http://link.aps.org/supplemental/10.1103/PhysRevLett.131.097001, which contains further details about theoretical modeling, device fabrication, experimental setup, device tune-up, extended data on the spin splitting versus gate voltage and magnetic field angle, as well as details of the spin-flip spectroscopy method, which also includes Refs. [47–59].

[47] C. Karrasch and V. Meden, Supercurrent and multiple singlet-doublet phase transitions of a quantum dot Josephson junction inside an Aharonov-Bohm ring, Phys. Rev. B **79**, 045110 (2009).

[48] I. Affleck, J.-S. Caux, and A. M. Zagoskin, Andreev scattering and Josephson current in a one-dimensional electron liquid, Phys. Rev. B **62**, 1433 (2000).

[49] A. V. Rozhkov and D. P. Arovas, Interacting-impurity Josephson junction: Variational wave functions and slave-boson mean-field theory, Phys. Rev. B **62**, 6687 (2000).

[50] E. Vecino, A. Martín-Rodero, and A. Levy Yeyati, Josephson current through a correlated quantum level: Andreev states and π junction behavior, Phys. Rev. B **68**, 035105 (2003).

[51] A. Oguri, Y. Tanaka, and A. C. Hewson, Quantum phase transition in a minimal model for the Kondo effect in a Josephson junction, J. Phys. Soc. Jpn. **73**, 2494 (2004).

[52] T. Meng, S. Florens, and P. Simon, Self-consistent description of Andreev bound states in Josephson quantum dot devices, Phys. Rev. B **79**, 224521 (2009).

[53] A. Bargerbos, W. Uilhoorn, C.-K. Yang, P. Krogstrup, L. P. Kouwenhoven, G. de Lange, B. van Heck, and A. Kou,

Observation of Vanishing Charge Dispersion of a Nearly Open Superconducting Island, Phys. Rev. Lett. **124**, 246802 (2020).
[54] A. Kringhøj, T. W. Larsen, B. van Heck, D. Sabonis, O. Erlandsson, I. Petkovic, D. I. Pikulin, P. Krogstrup, K. D. Petersson, and C. M. Marcus, Controlled dc Monitoring of a Superconducting Qubit, Phys. Rev. Lett. **124**, 056801 (2020).
[55] A. Kringhøj, L. Casparis, M. Hell, T. W. Larsen, F. Kuemmeth, M. Leijnse, K. Flensberg, P. Krogstrup, J. Nygård, K. D. Petersson, and C. M. Marcus, Anharmonicity of a superconducting qubit with a few-mode Josephson junction, Phys. Rev. B **97**, 060508(R) (2018).
[56] E. M. Spanton, M. Deng, S. Vaitiekénas, P. Krogstrup, J. Nygård, C. M. Marcus, and K. A. Moler, Current–phase relations of few-mode InAs nanowire Josephson junctions, Nat. Phys. **13**, 1177 (2017).
[57] S. Hart, Z. Cui, G. Ménard, M. Deng, A. E. Antipov, R. M. Lutchyn, P. Krogstrup, C. M. Marcus, and K. A. Moler, Current-phase relations of InAs nanowire Josephson junctions: From interacting to multimode regimes, Phys. Rev. B **100**, 064523 (2019).
[58] K. Serniak, S. Diamond, M. Hays, V. Fatemi, S. Shankar, L. Frunzio, R. J. Schoelkopf, and M. H. Devoret, Direct Dispersive Monitoring of Charge Parity in Offset-Charge-Sensitive Transmons, Phys. Rev. Appl. **12**, 014052 (2019).
[59] W. Uilhoorn, J. G. Kroll, A. Bargerbos, S. D. Nabi, C.-K. Yang, P. Krogstrup, L. P. Kouwenhoven, A. Kou, and G. de Lange, Quasiparticle trapping by orbital effect in a hybrid superconducting-semiconducting circuit, arXiv:2105.11038.
[60] C. Fasth, A. Fuhrer, L. Samuelson, V. N. Golovach, and D. Loss, Direct Measurement of the Spin-Orbit Interaction in a Two-Electron InAs Nanowire Quantum Dot, Phys. Rev. Lett. **98**, 266801 (2007).
[61] D. Liang and X. Gao, Strong tuning of Rashba spin–orbit interaction in single InAs nanowires, Nano Lett. **12**, 3263 (2012).
[62] J. A. van Dam, Y. V. Nazarov, E. P. A. M. Bakkers, S. D. Franceschi, and L. P. Kouwenhoven, Supercurrent reversal in quantum dots, Nature (London) **442**, 667 (2006).
[63] W. Chang, V. E. Manucharyan, T. S. Jespersen, J. Nygård, and C. M. Marcus, Tunneling Spectroscopy of Quasiparticle Bound States in a Spinful Josephson Junction, Phys. Rev. Lett. **110**, 217005 (2013).
[64] J. van Veen, D. de Jong, L. Han, C. Prosko, P. Krogstrup, J. D. Watson, L. P. Kouwenhoven, and W. Pfaff, Revealing charge-tunneling processes between a quantum dot and a superconducting island through gate sensing, Phys. Rev. B **100**, 174508 (2019).
[65] J. Koch, T. M. Yu, J. Gambetta, A. A. Houck, D. I. Schuster, J. Majer, A. Blais, M. H. Devoret, S. M. Girvin, and R. J. Schoelkopf, Charge-insensitive qubit design derived from the Cooper pair box, Phys. Rev. A **76**, 042319 (2007).
[66] A. Blais, R.-S. Huang, A. Wallraff, S. M. Girvin, and R. J. Schoelkopf, Cavity quantum electrodynamics for superconducting electrical circuits: An architecture for quantum computation, Phys. Rev. A **69**, 062320 (2004).
[67] A. Blais, A. L. Grimsmo, S. M. Girvin, and A. Wallraff, Circuit quantum electrodynamics, Rev. Mod. Phys. **93**, 025005 (2021).
[68] Precise gate voltage values for different gate configurations are reported in Ref. [46].
[69] J. J. Wesdorp, F. J. Matute-Cañadas, A. Vaartjes, L. Grünhaupt, T. Laeven, S. Roelofs, L. J. Splitthoff, M. Pita-Vidal, A. Bargerbos, D. J. van Woerkom, P. Krogstrup, L. P. Kouwenhoven, C. K. Andersen, A. Levy Yeyati, B. van Heck, and G. de Lange, Microwave spectroscopy of interacting Andreev spins, arXiv:2208.11198.
[70] We attribute the field-dependent change in flux dispersion to the renormalization of the impurity g factor by coupling to the leads, known as the impurity Knight shift [71].
[71] L. Pavešić, M. Pita-Vidal, A. Bargerbos, and R. Žitko, Impurity Knight shift in quantum dot Josephson junctions, arXiv:2212.07185.
[72] S. V. Sharov and A. D. Zaikin, Parity effect and spontaneous currents in superconducting nanorings, Physica E (Amsterdam) **29**, 360 (2005).
[73] Note that while all panels of Fig. 3 are measured at gate setpoint A of the quantum dot junction, Figs. 3(a) and 3(b) are measured at reference gate voltage $V_{\mathrm{J}} = 3860.0$ mV and Figs. 3(c) and 3(d) are taken at $V_{\mathrm{J}} = 4064.5$ mV.
[74] E. Strambini, A. Iorio, O. Durante, R. Citro, C. Sanz-Fernández, C. Guarcello, I. V. Tokatly, A. Braggio, M. Rocci, N. Ligato, V. Zannier, L. Sorba, F. S. Bergeret, and F. Giazotto, A Josephson phase battery, Nat. Nanotechnol. **15**, 656 (2020).
[75] L. Han, M. Chan, D. de Jong, C. Prosko, G. Badawy, S. Gazibegovic, E. P. A. M. Bakkers, L. P. Kouwenhoven, F. K. Malinowski, and W. Pfaff, Variable and Orbital-Dependent Spin-Orbit Field Orientations in an INSB Double Quantum Dot Characterized via Dispersive Gate Sensing, Phys. Rev. Appl. **19**, 014063 (2023).
[76] The tuning of the external flux requires a small magnetic field, which for the data in Fig. 4(a) ranges from −1.5 to 0.7 mT.
[77] X. Y. Jin, A. Kamal, A. P. Sears, T. Gudmundsen, D. Hover, J. Miloshi, R. Slattery, F. Yan, J. Yoder, T. P. Orlando, S. Gustavsson, and W. D. Oliver, Thermal and Residual Excited-State Population in a 3D Transmon Qubit, Phys. Rev. Lett. **114**, 240501 (2015).
[78] A. A. Kiselev, E. L. Ivchenko, and U. Rössler, Electron g factor in one- and zero-dimensional semiconductor nanostructures, Phys. Rev. B **58**, 16353 (1998).
[79] S. Csonka, L. Hofstetter, F. Freitag, S. Oberholzer, C. Schönenberger, T. S. Jespersen, M. Aagesen, and J. Nygård, Giant fluctuations and gate control of the g-factor in InAs nanowire quantum dots, Nano Lett. **8**, 3932 (2008).
[80] M. D. Schroer, K. D. Petersson, M. Jung, and J. R. Petta, Field Tuning the g Factor in InAs Nanowire Double Quantum Dots, Phys. Rev. Lett. **107**, 176811 (2011).
[81] G. W. Winkler, D. Varjas, R. Skolasinski, A. A. Soluyanov, M. Troyer, and M. Wimmer, Orbital Contributions to the Electron g Factor in Semiconductor Nanowires, Phys. Rev. Lett. **119**, 037701 (2017).
[82] J. Linder and J. W. A. Robinson, Superconducting spintronics, Nat. Phys. **11**, 307 (2015).
[83] Y. M. Shukrinov, Anomalous Josephson effect, Phys. Usp. **65**, 317 (2022).
[84] A. Bargerbos, 4TU.ResearchData, 10.4121/c.6076818.v2.